GOSPODARKA SUROWCAMI MINERALNYMI

Tom 24 2008 Zeszyt 4/1

JAROSŁAW ŚLIZOWSKI*, JAN WALASZCZYK**

Long term stability evaluation of natural gas storage caverns

Introduction

Underground natural gas storage in caverns leached in rock salt formations with the application of a bore-hole method is one of three gas storage techniques. The method relies on water injection into a borehole and extraction of brine. The two other storage techniques make use of empted reservoirs of oil and gas formation and water-bearing horizons.

The main advantages of storage caverns, comparing to the other storage facilities, are: much higher capability of possible gas output and smaller risk that some of storage medium will be inaccessible in the future. Disadvantage is higher cost of their construction.

The design of storage cavern requires determination of cavern size and shape as well as maximal and minimal gas storage pressure to assure a long term stability of the cavern.

Several stability aspects have been considered like: massif strength ratio at the cavern wall as well as the range of cavern influence, tightness and convergence.

In the design phase, the caverns are of an axisymmetric shape. Such an assumption is entirely correct in the case of homogenous or horizontally layered massif, which occurs in bedded deposits. In the case of salt domes, where layers were tilted at a steep angle, caverns shape usually differs from axisymmetric, but anyhow it is impossible to determine the eventual cavern shape in the design phase.

Due to above mentioned conditioning as well as to lack of recognition of salt massif mechanical properties, so far there was no unambiguously obligated method of natural gas storage cavern designing in salt formations. The method of caverns stability evaluation

* Ph.D.Sc. Eng., Mineral and Energy Economy Research Institute of Polish Academy of Sciences, Kraków, Poland; e-mail: slizow2@min-pan.krakow.pl

** Professor, AGH-University of Science and Technology, Faculty of Mining and Geoengineering, Kraków, Poland.

presented in the article includes analysis of different models of an axisymmetric cavern vary with creep law coefficients values and boundary conditions. Two different scenarios of cavern exploitation and different massif strength ratio criteria have been considered.

1. Numerical models of storage cavern

1.1. Shape and boundary conditions of cavern models

The calculation included two axisymmetric models of cavern shown in figure 1.

The analyzed cavern is a cylinder with diameter of 70 m, ended by spherical dome at the roof and at the bottom. Cavern roof is located 1000 m deep, the bottom 1250 m. It is an idealized shape and being such it does not correspond precisely to anyone of KPMG Mogilno caverns, however is often used in stability evaluation at the project phase (Lux, Hou, Düsterloh 1998).

The value of specific gravity of overlaid rocks, above calculation model used in the calculation was $\gamma_{sk} = 21.57$ kN/m^3, specific gravity of salt $\gamma_{so} = 21.18$ kN/m^3 and temperature gradient 0.03°C/m. The values correspond to average conditions of Polish salt domes.

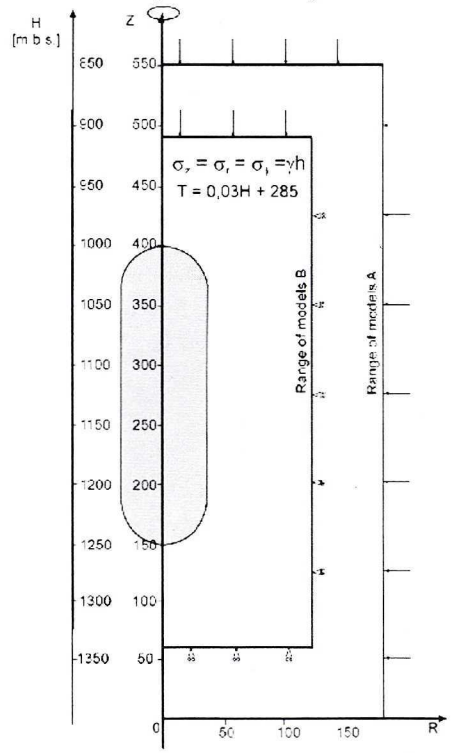

Fig. 1. Location, shape and boundary conditions of cavern models

Rys. 1. Lokalizacja i kształt komory oraz warunki brzegowe w rozważanych modelach

Two variants of boundary condition corresponding to extreme states of caverns interaction have been considered.

Variant A – corresponds to an isolated single cavern i.e. with no interaction with other caverns. Thus at the boundary of the model, 150 m distant from the cavern wall (185 m from the cavern axis) natural lithostatic pressure have been assumed.

Variant B – corresponds to maximal possible caverns interaction. Caverns are placed in net of module 250 m, thus at the boundary of the model 125 m distant of the cavern axis, no radial displacement have been assumed.

1.2. Creep law applied in the analysis

In the calculation superposition of elastic, plastic and viscous strains have been applied. The biggest influence on the results has creep law describing viscous strains. Norton creep law, still most commonly used, was applied in the analysis:

$$\dot{\varepsilon}^{v}_{ef} = A\mathrm{e}^{-\frac{Q}{RT}}\sigma^{n}_{ef} \tag{1}$$

where:

- $\dot{\varepsilon}^{v}_{ef}$ – effective creep strain rate [d^{-1}],
- σ_{ef} – effective stress [MPa],
- Q – free activation energy [$J \cdot mol^{-1}$],
- R – gas constant – 8.3144 $J \cdot mol^{-1} \cdot K^{-1}$ = 1.987 $cal \cdot mol^{-1} \cdot K^{-1}$,
- T – temperature [K],
- A – coefficient in Norton law [d^{-1}],
- n – power exponent in Norton law [–].

In the case of stress and strain distribution analysis around the cavern placed at definite depth the most significant is influence of exponent "*n*". Four values of "*n*" were used for the calculations and the basic variants were of extreme values.

The same value of 5750K was taken for coefficient Q/R in all calculated variants. Parameter A was adopted in such way, to obtain for every n the same creep rate – 0.02‰/day at effective stress σ_{ef} = 10 MPa and temperature T = 50°C (temperature at the cavern centre). It is relatively high rate, characteristic for coarse-grained salt. Table 1 contains sets of all Norton law coefficients used in the calculation.

Strain rates corresponding to the creep law variants used in the calculation are shown in figure 2.

Values of exponent n adopted here, cover the whole range of values known from the literature with one exception (Hunshe, Hampel 1999) were value of exponent n was assessed being equal to 7.0.

TABLE 1

Norton creep law coefficient values

TABELA 1

Wartości współczynników prawa pełzania Nortona

Set	A [d^{-1}]	n	Q/R [K]	Line symbols on figures
1	1.91550	2.75	5750	———
2	0.10772	4.00		– · – · – · –
3	$1.915 \cdot 10^{-2}$	4.75		– – – – – –
4	$3.41 \cdot 10^{-3}$	5.50		.....

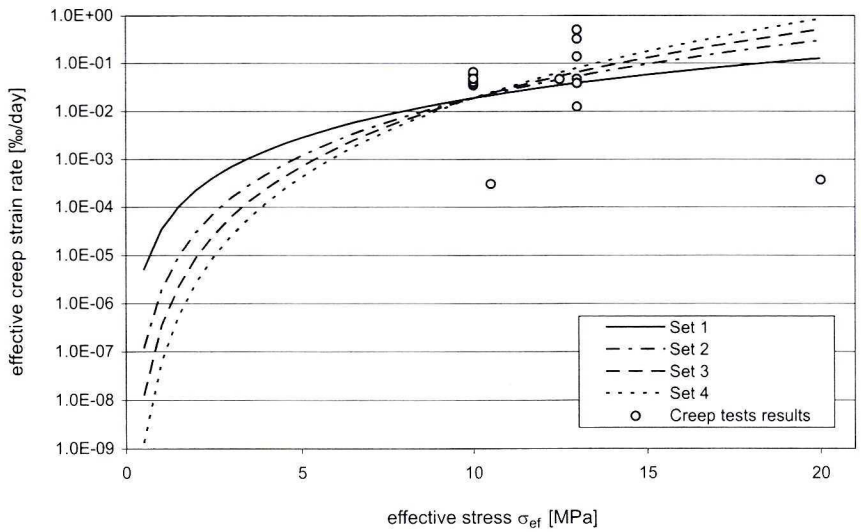

Fig. 2. Stationary creep rate at a temperature 50°C according to considered creep laws

Rys. 2. Prędkość pełzania stacjonarnego w temperaturze 50°C według rozważanych praw pełzania

1.3. Numerical simulation scenarios and models symbols

Two kinds of cavern loading scenarios were simulated. First scenario for theoretical purposes, aimed to determine internal cavern pressure influence on distribution of stress and strain rate around the cavern in stationary conditions.

First simulation was determined for cavern filled with brine. Saturated brine density 11.77 kN/m^3 and the cavern depth gave brine pressure of 11.8 MPa at the cavern roof and 14.7 MPa at the bottom.

Next internal pressure was diminished in 4 stages, successively to 7 MPa, 4 MPa, 2 MPa and 0 MPa. Then the pressure was increased in 6 stages successively to 2 MPa, 4 MPa,

7 MPa, 10 MPa, 14 MPa i 18 MPa. Two year simulation was determined for each of 11 stages.

Maximal value of gas pressure is determined by microfracturing tests of massif, which are carried out in boreholes.

Second scenario corresponds to real storage caverns exploitation plan (Ślizowski, Urbańczyk 2003). It divides yearly cycle of the cavern operation into 4 stages:

— 30 days of gas withdrawal,

— 150 days of idle with minimum operational pressure,

— 30 days of gas injection,

— 200 days of idle with maximal operational pressure.

Maximal storage pressure taken for the calculation was P_{max} = 18 MPa, resulting from microfracturing gradient determined in boreholes, and minimal storage pressure P_{min} = 4 MPa which was determined based on scenario 1 simulation outcome.

The second scenario calculations began with 4-years long period of cavern filled with brine, followed by first filling and next 5 full cycles of filling and unloading simulations.

Finally, the range of the calculations consisted of several different models referenced below by the symbol **Model Xm.n.**, where:

X – A or B depending on variant,

m – number of creeping law parameters set (1–4),

n – number of scenario (1 or 2).

Actually, for scenario 1, calculation for border values of exponent "n" were performed providing 4 models referenced as A1.1, A4.1, B1.1, B4.1. For scenario 2 calculations for all possible variants combinations were performed providing 8 models referenced as A1.2, A2.2, A3.2, A4.2, and B1.2, B2.2, B3.2, B4.2.

2. Massif strength and range of cavern influence estimation

2.1. Stress and effective strain rate distribution according to first scenario

Effective stress and effective strain rate at the roof and wall of storage cavern according to first scenario of simulation are presented in figure 4 and 5.

Qualitatively all distributions at the cavern roof and cavern wall are similar. At the first stages of simulation where internal cavern pressure was decreased, both effective stress and effective strain rates decrease in time and effect diminish with pressure. Opposite effect is observed in the case of increased internal pressure. Both analyzed quantities increase with time, and stress increase each stage is bigger.

Next important feature of obtained distributions is the fact, that for given internal cavern pressure, analyzed quantities stabilize at the same value independently whether pressure was

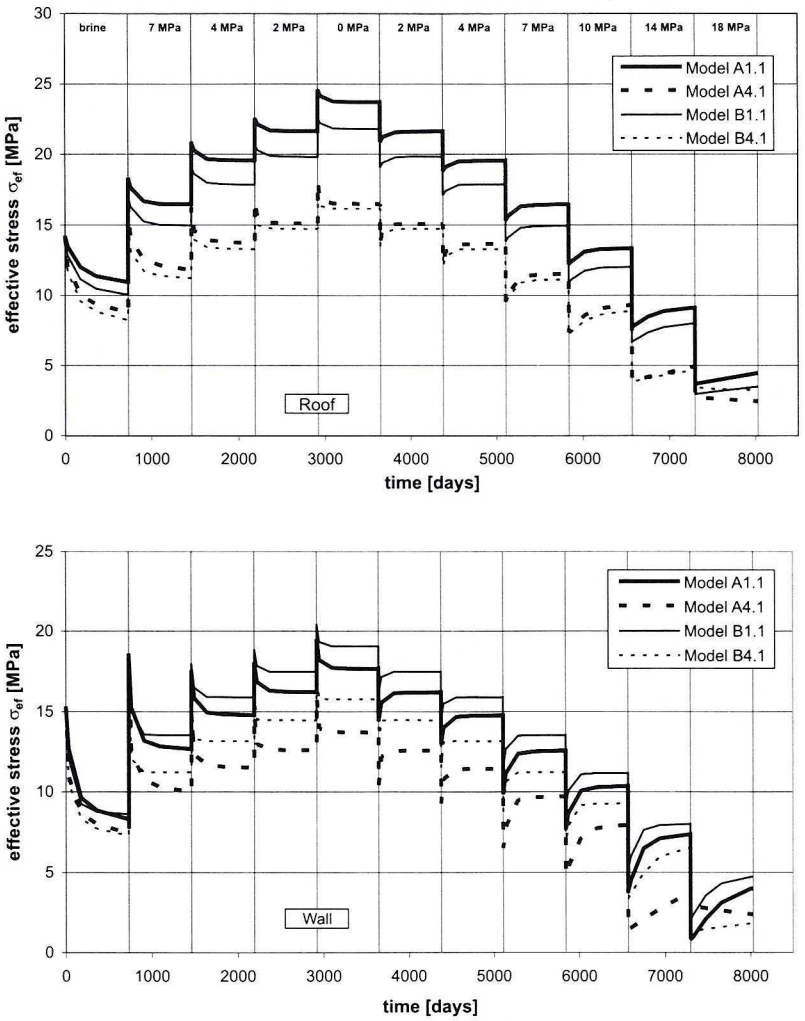

Fig. 3. Effective stress at the roof and wall of storage cavern according to scenario 1

Rys. 3. Naprężenie efektywne w stropie i na ociosie komory według scenariusza 1

increased or decreased. E.g for 4 MPa, asymptotic value of effective stress is the same both for 3 and 7 stage.

From the quantitative point of view, the situation is more complicated and depends which quantity is taken into account.

In the case of effective stress, one can observe, that stresses at the cavern wall have smaller value for set 4 of creep parameters (the highest n). It concerns both model A and B. Such effect can be expected, the higher value of "n", the better ability to reduce the extreme stresses. Interesting is the fact, that the above relation is observed even for high values of internal cavern pressure, when effective stresses are below 10 MPa and creep rate for set 4 of creep parameters is smaller than for set 1.

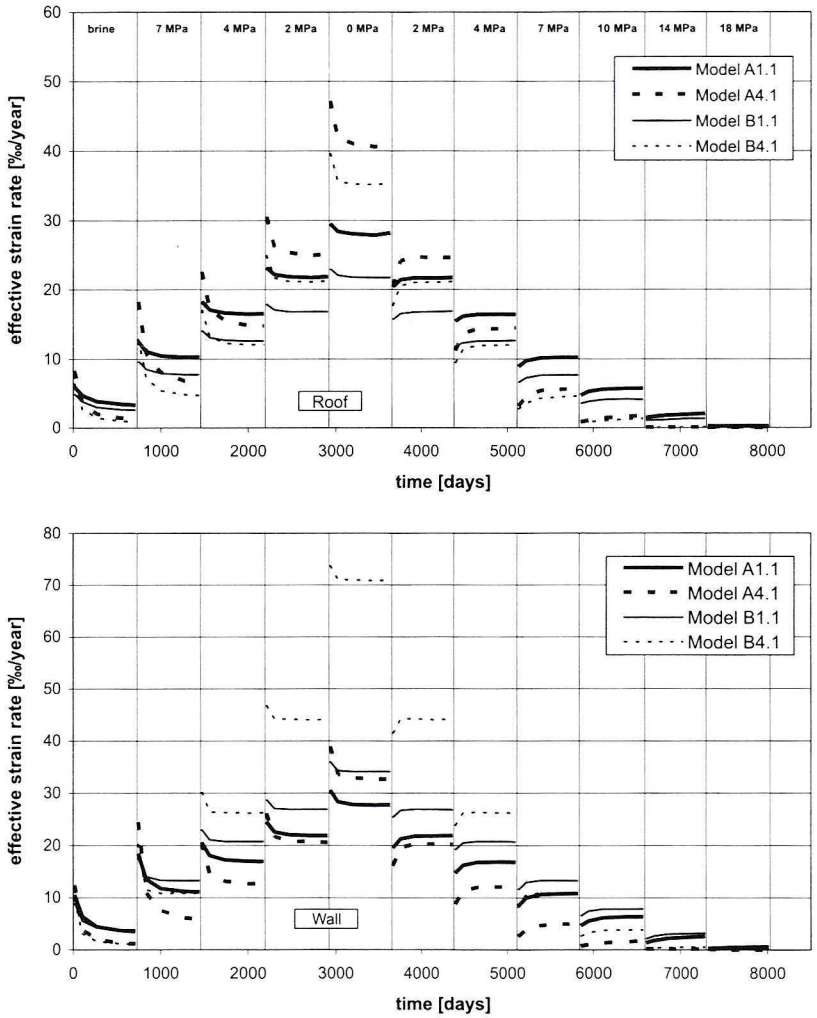

Fig. 4. Effective strain rate at the roof and wall of storage according to scenario 1

Rys. 4. Prędkość odkształceń efektywnych w stropie i na ociosie komory według scenariusza 1

In the case of strains, one could expect opposite effect. i.e. that strain rate is higher for model giving higher value of creep rate. It is not generally valid in every case, e.g. for internal pressure of 7 MPa, higher value of strain rate is obtained in the case of set 1, both at the cavern roof and cavern wall.

It means, that sometimes effect of stress reduction is stronger than differences between creep rates of analyzed creep laws.

According to theoretical scenario, steady-state stress and strain rate distribution at the end of each stages are the most important for cavern stability estimation. Distributions obtained at internal pressure of 4MPa (value adopted as a minimal storage pressure at 2.2 chapter) are presented in figure 5 and 6, values at the cavern roof and cavern wall are collected in table 2.

TABLE 2

Effective stress, effective strain rate and effort coefficients in cavern roof and wall

TABELA 2

Wartości naprężeń efektywnych, prędkości odkształceń efektywnych i współczynników wytężenia górotworu w stropie i na ociosie

Pressure	Model	Roof				Wall			
		σ_{ef} [MPa]	$\dot{\varepsilon}_{ef}$ [‰/year]	$W_{\sigma_1^{max}}$	W_B	σ_{ef} [MPa]	$\dot{\varepsilon}_{ef}$ [‰/year]	$W_{\sigma_1^{max}}$	W_B
7 MPa	A1.1	16.46	10.29	0.279	0.241	12.66	11.06	0.242	0.182
	A2.1	11.82	6.46	0.225	0.151	9.99	5.77	0.210	0.128
	B1.1	14.95	7.74	0.263	0.212	13.52	13.27	0.253	0.195
	B2.1	11.22	4.74	0.220	0.141	11.21	10.83	0.224	0.150
4 MPa	A1.1	19.58	16.53	0.359	0.357	14.78	16.94	0.307	0.281
	A2.1	13.72	14.77	0.276	0.228	11.51	12.54	0.254	0.202
	B1.1	17.87	12.63	0.337	0.321	15.89	20.70	0.324	0.299
	B2.1	13.30	12.09	0.272	0.221	13.16	26.19	0.281	0.237
2 MPa	A1.1	21.65	21.87	0.454	0.450	16.22	21.89	0.393	0.371
	A2.1	15.11	25.14	0.345	0.299	12.59	20.56	0.320	0.275
	B1.1	19.84	16.83	0.427	0.410	17.48	26.87	0.416	0.389
	B2.1	14.73	21.23	0.341	0.293	14.47	44.18	0.357	0.317
0 MPa	A1.1	23.72	28.16	0.658	0.557	17.67	27.70	0.640	0.489
	A2.1	16.50	40.89	0.509	0.387	13.70	32.67	0.528	0.378
	B1.1	21.79	21.79	0.622	0.515	19.06	34.09	0.669	0.501
	B2.1	16.16	35.35	0.506	0.383	15.77	70.95	0.582	0.423

Differences between the models are significant and not only related to external stress reduction. Comparing obtained stress distribution one can observe different ranges of cavern influence. Simple relation occurs; higher decrease of effective stress at the cavern wall induces higher increase of effective stress inside the model. In consequence, considering stress state, the range of cavern influence depends basically on creep law. In the case of strain analysis the major influences on the range of cavern influence have variants A or B.

2.2. Rock massif strength ratio evaluation

Apart from effective stress and strain, massif strength ratio at two points – cavern roof and cavern wall was analyzed.

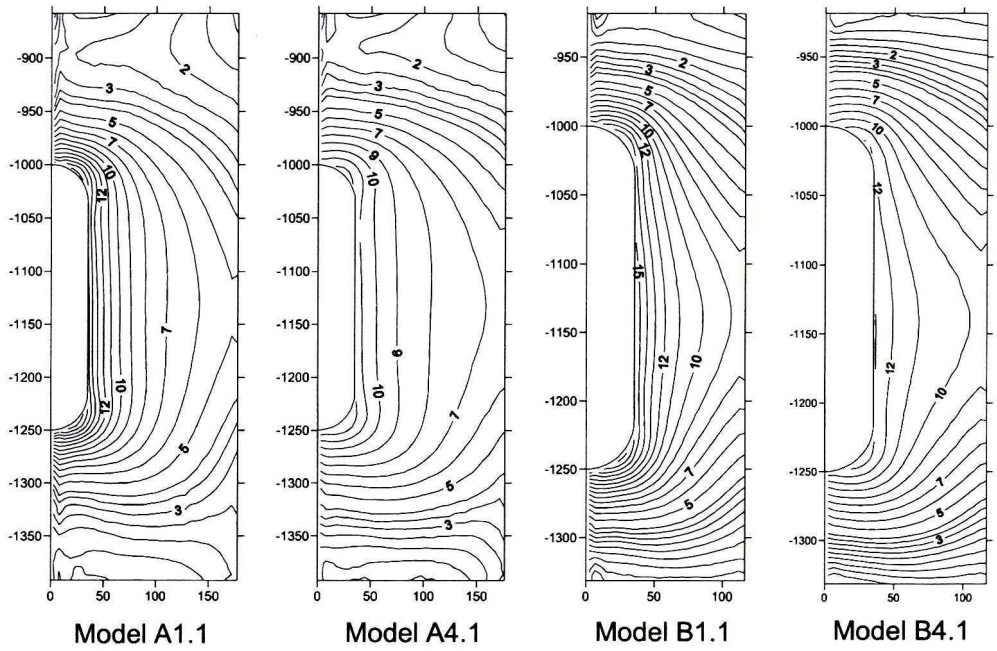

Fig. 5. Effective stress (stationary) σ_{ef} [MPa] – gas pressure 4 MPa

Rys. 5. Naprężenie efektywne (ustabilizowane) σ_{ef} [MPa] – ciśnienie gazu 4 MPa

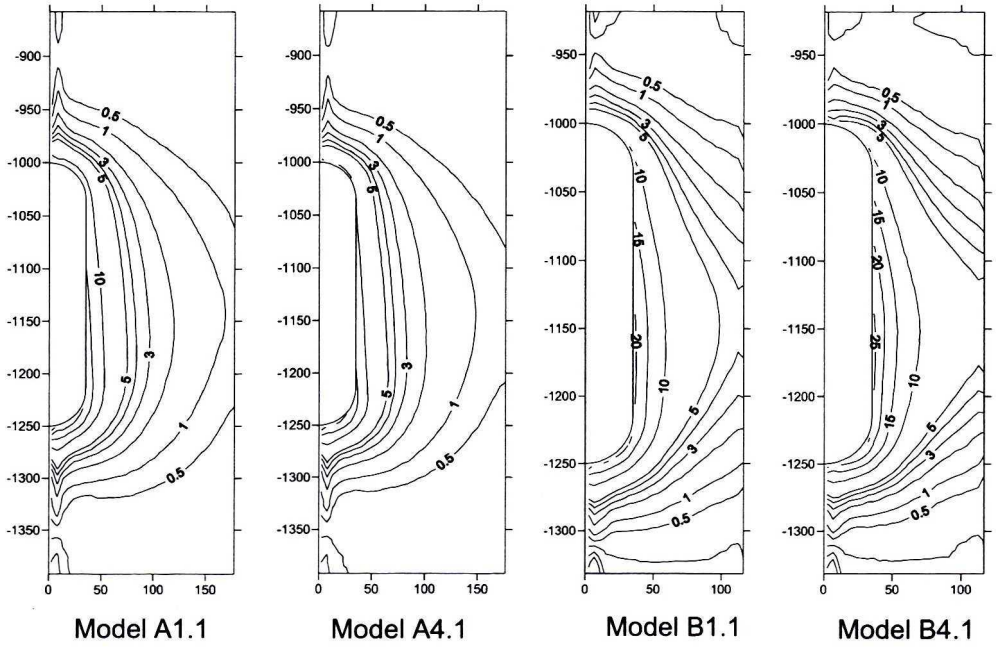

Fig. 6. Effective strain rate $\dot{\varepsilon}_{ef}$ [‰/year] – gas pressure 4 MPa

Rys. 6. Prędkość odkształceń efektywnych $\dot{\varepsilon}_{ef}$ [‰/rok] – ciśnienie gazu 4 MPa

In the case of first scenario, two effort coefficients have been considered:

— $W_{\sigma_1^{max}}$ given by the equations

$$W_{\sigma_1^{max}} = \frac{\sigma_1}{\sigma_1^{max}} \tag{2}$$

$$\sigma_1^{max} = a\sigma_3^b + R_c \tag{3}$$

where: R_c = 20.6; a = 17.55; b = 0.692

— W_B given by the equation

$$W_B = \frac{1}{2\alpha R_c}\left[3(\alpha-1)\sigma_m + \sqrt{9(\alpha-1)^2\sigma_m^2 + 4\alpha\sigma_{ef}^2}\right] \tag{4}$$

where: R_c = 20.6; α = 0.025

The case where values of coefficients $W_{\sigma_1^{max}}$ and W_B are below 0.3 is assumed to be entirely safe, whereas situation is unacceptable when values exceed 0.4 (Ślizowski, Urbańczyk 2004).

In the case of second scenario strain criterion with $W_{\varepsilon_1^{max}}$ coefficient given by the following equation have been considered

$$W_{\varepsilon_1^{max}} = \frac{\varepsilon_1}{\varepsilon_1^{max}} \tag{5}$$

$$\varepsilon_1^{max} = c\sigma_3^d + \varepsilon_0^{kr} \tag{6}$$

where:

ε_0^{kr} = 30 [‰]; c = 21.82 [‰]; d = 0.74

A case is assumed entirely safe when value of coefficient $W_{\varepsilon_1^{max}}$ is below 1. It is related to the fact that in long-term load tests, destructive load reaches at least the same value as in short-term tests for which external value of ε_1^{max} has been determined.

Maximal axial stress and strain values given by triaxial compression tests in accordance with above criteria are shown in figures 7 and 8.

Values massif strength ratio at the cavern wall according to above criteria are listed in table 2.

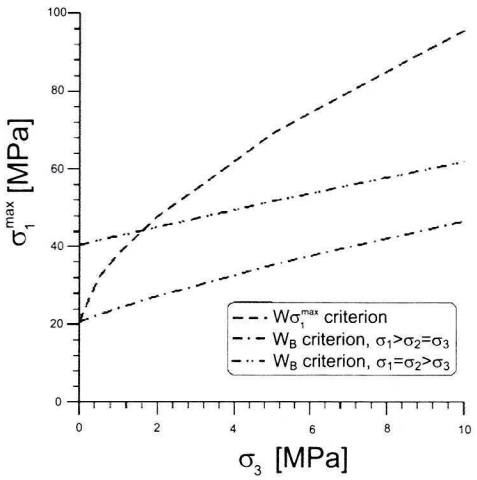

Fig. 7. Ultimate principal stress (axial and confining) vs. minimal stress in triaxial tests

Rys. 7. Maksymalne naprężenie główne (osiowe lub boczne) w zależności od naprężenia minimalnego według rozpatrywanych kryteriów, w warunkach trójosiowego stanu naprężeń

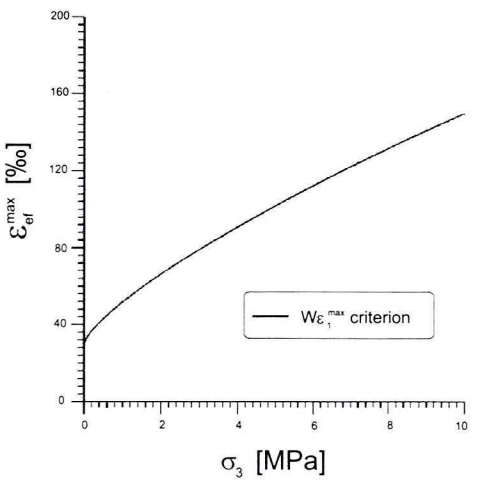

Fig. 8. Ultimate effective strain vs. minimal stress in triaxial tests

Rys. 8. Maksymalne odkształcenie efektywne w zależności od naprężenia minimalnego według kryterium odkształceniowego w warunkach trójosiowego stanu naprężeń

Different values of effective stress affect differences in analyzed massif strength coefficients, which also significantly differs each other in particular point.

On the basis of considered criteria it can be concluded that minimal storage pressure which guarantees cavern stability is 4 MPa. Due to much higher values of coefficient an entire cavern unload is unacceptable. Also pressure decrease to 2 MPa value is unsafe because values of some coefficients are higher than 0.4. Following minimal storage pressure value taken for second scenario calculation was 4 MPa.

2.3. Stress and effective strain rate estimation according to second scenario

Distributions of effective stress in successive years of exploitation scenario were comparable. For that reason, the results of calculations presented in figure 9 separately for models A and B are limited to one year.

In the case of minimal pressure, similarly to the first scenario effective stress values are inversely proportional to "n" coefficient. The opposite situation occurs in the case of maximal pressure, higher coefficient "n" value gives higher effective stress.

Nevertheless, the major purpose of the calculations in accordance with second scenario was determining of actual massif deformation rate.

Effective strain value at the cavern wall for the whole simulation is show in figure 10.

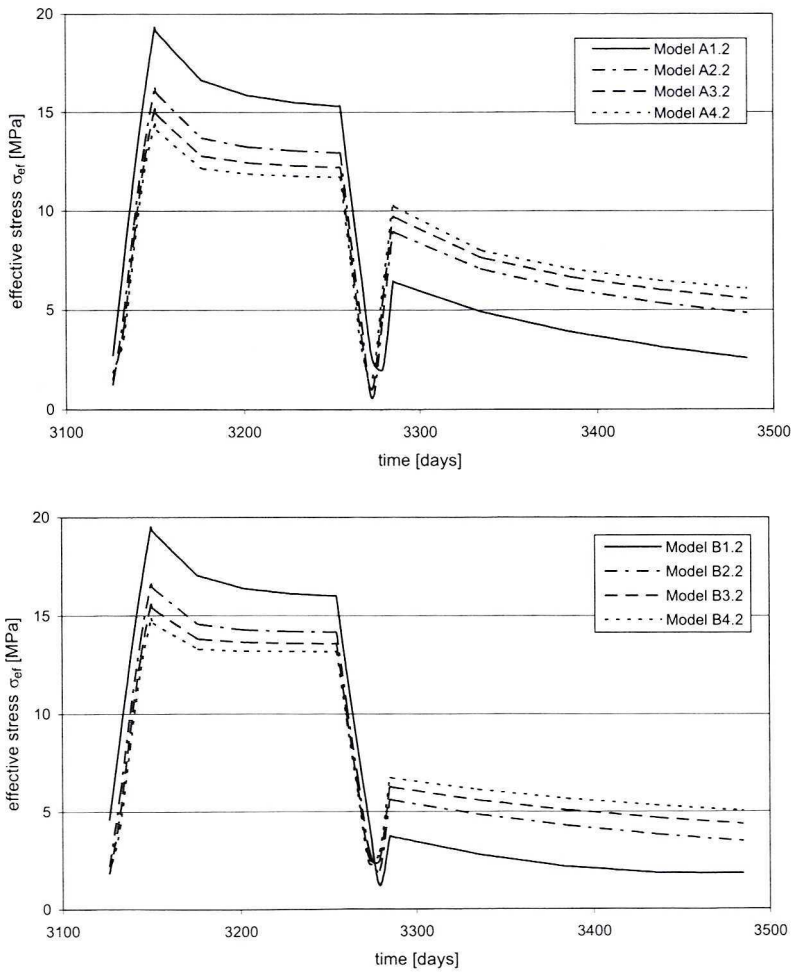

Fig. 9. Effective stress at the cavern wall during the last year of simulation according to scenario 2

Rys. 9. Naprężenie efektywne na ociosie komory w ostatnim roku symulacji według scenariusza 2

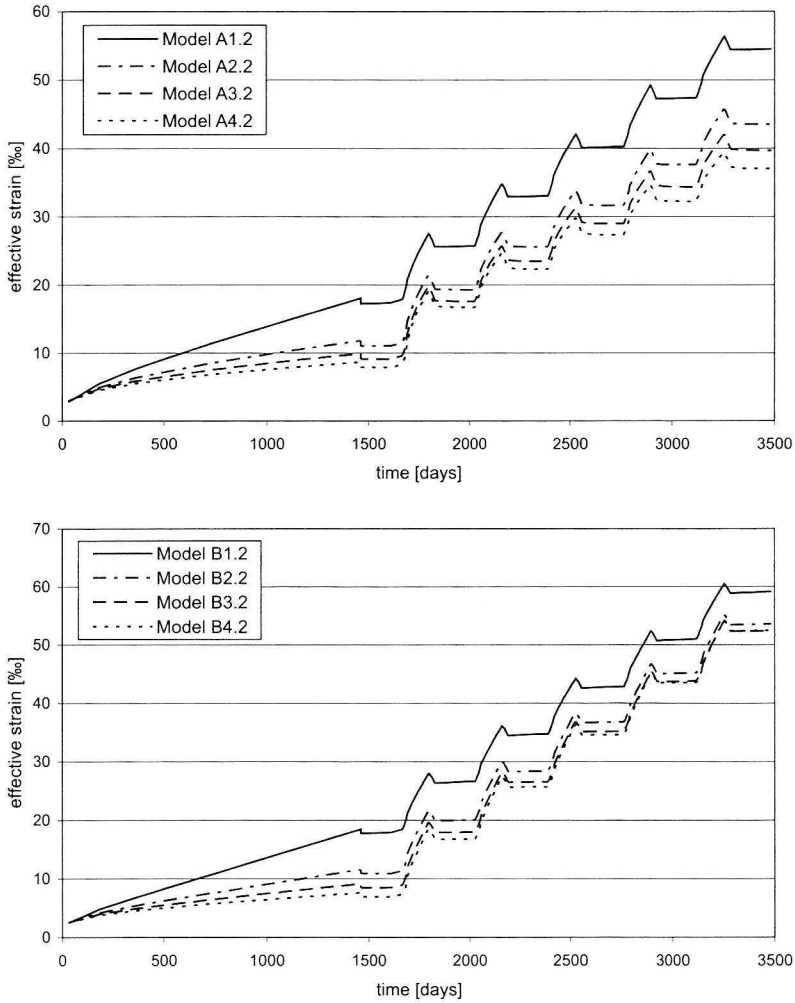

Fig. 10. Effective strain at the cavern wall

Rys. 10. Odkształcenia efektywne na ociosie komory

Annual increases of effective strain obtained by simulation and annual increases of $W_{\varepsilon_1^{max}}$ coefficient for extreme values of "n" coefficient are listed in table 3.

Annual increases indicates that value of $W_{\varepsilon_1^{max}}$ will not exceed 1 during at least 20 years, and for the most of the models this period is above 30 years.

However, there are some doubts regarding maximal storage pressure. Figure 11 shows axial stress values at the depth of cavern centre after filling with maximal pressure.

For all of the models in the cavern vicinity stress values decrease much below 18 MPa, which can unable migration of gas. The range of stress decrease depends on the model taking for calculation besides the research works upon gas migration process are being carried out.

TABLE 3

Annual increases of effective strain and coefficients $W_{\varepsilon_1^{max}}$

TABELA 3

Roczne przyrosty odkształceń efektywnych i współczynników $W_{\varepsilon_1^{max}}$

Model	Strain increment [‰/year]		$W_{\varepsilon_1^{max}}$ increment [year^{-1}]	
	roof	wall	roof	wall
A1.2	6.43	7.12	0.0314	0.0369
A4.2	5.47	4.79	0.0353	0.0304
B1.2	4.75	8.13	0.0245	0.0403
B4.2	4.08	8.93	0.0265	0.0517

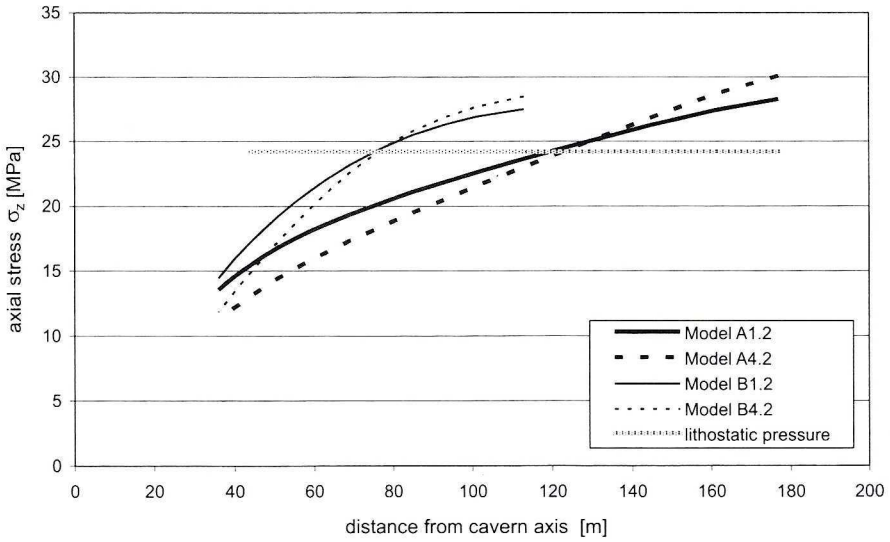

Fig. 11. Distribution of axial (vertical) stress at the depth of cavern's center

Rys. 11. Rozkład naprężeń osiowych (pionowych) na głębokości środka komory

3. Cavern convergence

Values of relative convergence obtained from simulation of second scenario are presented in the figure 12.

Similarly to effective stress, relation between cavern convergence and creep law occurs. As shown in figure 12, the higher value of "n" coefficient, the lower value of convergence. For annual convergence (see table 4), this is valid for models of kind A. For models of kind B, where higher values of convergence were obtained, the situation is opposite.

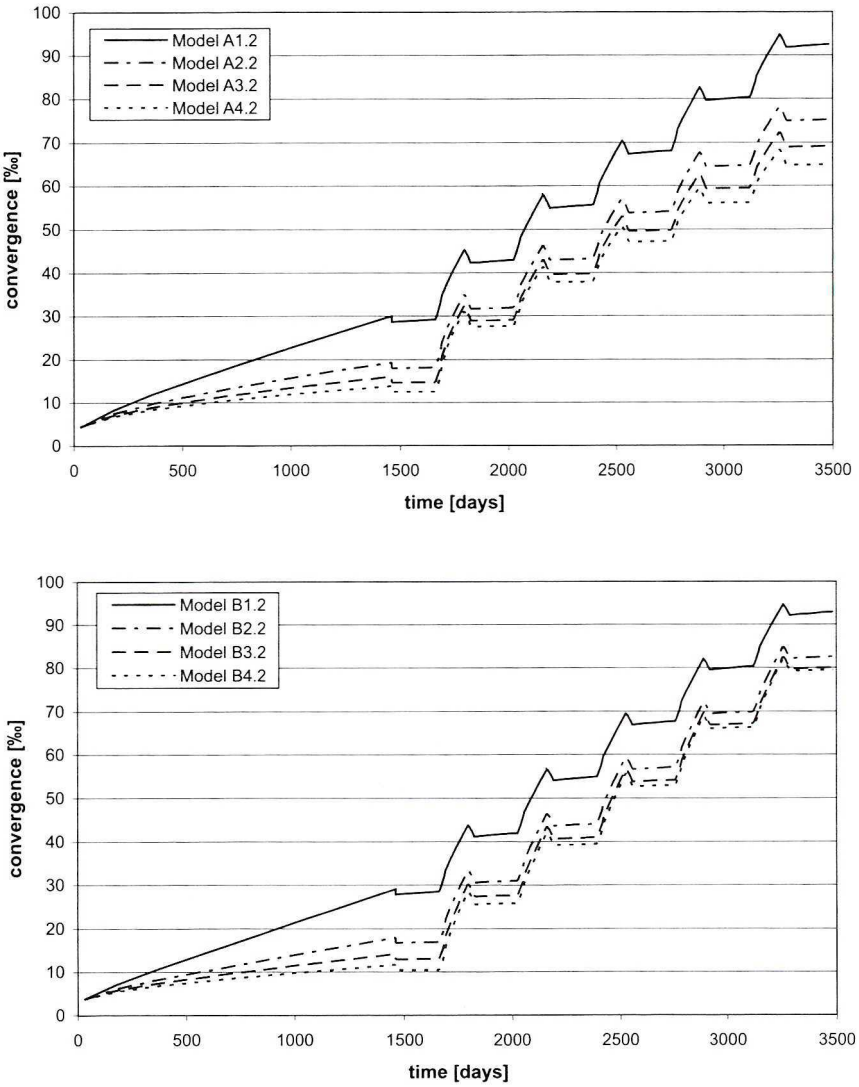

Fig. 12. Cavern convergence according to scenario 2

Rys. 12. Konwergencja komory według scenariusza 2

Such effect must be related to the fact, that convergence is a result of strains of entire analyzed area, i.e zones of effective stress lower than 10 MPa and zones of effective stress higher than 10 MPa (for 10 MPa the creep rate is equal for all parameters set taken into account).

The significant influence on cavern convergence has minimal storage pressure. Analysis of massif strength ratio showed that in the case of the Mogilno caverns places in homogenous rock, it is possible to decrease minimal pressure value. Detailed analysis of cavern exploitation scenario will show whether this is profitable from the convergence point of view.

TABLE 4

Annual increases of storage cavern convergence according to scenario 2

TABELA 4

Roczne przyrosty konwergencji według scenariusza 2

Years	Relative convergence yearly [‰]							
	model A1.2	model A2.2	model A3.2	model A4.2	model B1.2	model B2.2	model B3.2	model B4.2
1	13.8	13.9	14.4	15.2	13.5	14.2	14.7	15.4
2	12.7	11.3	10.7	10.2	12.9	13.1	13.3	13.6
3	12.4	10.8	10.0	9.3	12.8	12.9	13.1	13.5
4	12.3	10.6	9.7	8.9	12.7	12.8	13.0	13.3
5	12.2	10.5	9.6	8.7	12.6	12.7	12.9	13.2

Summary

To determine the exploitation parameters of gas storage cavern one should take into account diversity of mining-geological conditions. Because of the fact, that in the design phase recognition of salt dome geology is limited, it is recommended to consider extreme variants.

Analysis of different variants of axisymmetric models confirmed that decrease of extreme stress at the cavern wall depends mostly on the exponent "n" of exponential function which determines stress influence on creep rate in Norton law. Higher values of the exponent cause higher decrease of effective stress at the cavern wall, which induces higher increase of effective stress inside the model and consequently increase of the cavern influence range.

The next result of stress decrease is fact that cavern convergence is not proportional to the value of exponent "n", as one could expect, but in the case of A models even the opposite effect occurred.

The calculations showed that known from literature tendency to use high values of exponent "n" can not be treated as the most safe cavern stability evaluation.

REFERENCES

Hunshe U., Hampel A., 1999 – Rock-salt – the mechanical properties of the host rock material for a radioactive waste repository. Engineering Geology 52, s. 271–291.

Lux K.-H., Hou Z., Düsterloh U., 1998 – Some New Aspects in Modelling of Cavern Behavior and Safety Analysis. SMRI Meeting 4–7, Octtober 1998, Rome, Italy.

Ślizowski J., Urbańczyk K., 2004 – Influence of depth on rock salt around the single chamber. IGSMiE, Kraków.

Ślizowski J., Urbańczyk K., 2003 – Prognozowanie konwergencji względnej komory magazynowej gazu ziemnego przy zastosowaniu zaktualizowanego modelu górotworu solnego. IGSMiE PAN, Kraków, Gosp. Sur. Min. t. 19, z. 2. s. 43–56.

OCENA DŁUGOTRWAŁEJ STATECZNOŚCI KOMÓR MAGAZYNOWYCH GAZU ZIEMNEGO

Słowa kluczowe

Podziemne magazynowanie, wytężenie górotworu solnego, konwergencja

Streszczenie

Magazynowanie gazu ziemnego w komorach solnych jest najefektywniejszym sposobem podziemnego magazynowania tego surowca. Warunki geologiczno-górnicze występujące w polskich wysadach solnych nie są niestety jednoznacznie korzystne, co powoduje konieczność indywidualnego wyznaczania parametrów każdej komory. Analizując stateczność konkretnej komory należy zwrócić uwagę na takie zagadnienia jak: wytężenie górotworu na brzegu komory, zasięg jej oddziaływania oraz prędkość konwergencji w zależności od scenariusza eksploatacji, a w szczególności od wartości minimalnego i maksymalnego ciśnienia magazynowania.

W artykule analizowano te zagadnienia na przykładzie teoretycznej komory odpowiadającej, pod względem warunków brzegowych, przeciętnym komorom magazynowym gazu eksploatowanym w wysadzie solnym Mogilno.

Największy wpływ na stateczność komory mają nierozpoznane dotychczas właściwości reologiczne górotworu solnego, w związku z tym w artykule uwzględniono 4 różne zestawy parametrów prawa pełzania Nortona użytego w modelach. Rozważono 2 warianty obciążenia modelu odpowiadające minimalnemu i maksymalnemu oddziaływaniu komór sąsiednich. Obliczenia obejmowały 2 scenariusze eksploatacji komory: teoretyczny, którego celem było określenie wartości minimalnego ciśnienia magazynowania oraz scenariusz odpowiadający rzeczywistemu harmonogramowi eksploatacji komór.

Wobec braku jednoznacznego kryterium opisującego długotrwałą wytrzymałość soli kamiennej, wytężenie górotworu na brzegu komory oceniono na podstawie 3 niezależnych kryteriów.

Analiza wyników wskazuje, że większy wpływ na rozkład naprężeń górotworu w otoczeniu komory ma przyjęte prawo pełzania niż warunki brzegowe. Obliczenia wykazały również, że przyjmowanie wysokiej wartości potęgi opisującej wpływ naprężeń w prawie pełzania Nortona nie stanowi bezpiecznego oszacowania prędkości odkształceń górotworu i konwergencji oraz wskazały, że zeszczelinowanie górotworu może nastąpić przy ciśnieniu niższym niż wynika to z prób mikroszczelinowania przeprowadzonych w otworach wiertniczych.

Bez względu na powyższe w przypadku komór w wysadzie Mogilno zlokalizowanych w jednorodnej warstwie możliwe jest obniżenie wartości minimalnego ciśnienia magazynowania w porównaniu z aktualnie obowiązującymi projektami technicznymi. Stwierdzenie czy jest to opłacalne z punktu widzenia długotrwałej efektywnej pojemności magazynu wymaga przeanalizowania szczegółowego scenariusza eksploatacji rozpatrywanej komory.

Key words

Underground storage, rock salt massif effort, convergence

Abstract

Underground natural gas storage in salt caverns is the most efficient method of gas storage. Since geological and mining-engineering conditions of Polish rock-salt formations are not favourable, it is essential to specify technical parameters for each cavern independently. Stability assessment of particular cavern should include the following issues: rock salt massif strength ratio at the cavern wall, range of cavern influence and rate of cavern convergence depending on cavern loading scenario and mostly on minimal and maximal storage pressure.

The paper presents analysis of the above mentioned aspects on the example of hypothetical cavern, in the case of boundary conditions, similar to typical gas storage cavern being operated in the Mogilno salt dome.

The major influence on cavern stability have undefined so far rheological properties of rock salt massif, therefore in the article 4 different sets of Norton creep law parameters used in models have been analyzed. Two variants of model load, corresponding to minimal and maximal interaction of neighbouring caverns have been considered. The calculations included two kinds of cavern loading scenarios: scenario for theoretical purposes, aimed to define minimal storage pressure and scenario typical to storage cavern operation.

Due to lack of explicit criteria describing long term stability of rock salt, rock salt massif strength ratio at the cavern wall was estimated on the basis of 3 independent criteria.

Analysis of the calculation results showed that greater influence on stress-strain distribution of rock salt massif demonstrate creeping low, than boundary conditions. Besides, the high value of power coefficient describing stress influence in Norton creep law is not safe to estimate strain rate of rock-salt massif and cavern convergence. The calculations pointed out that micro-fracturing process in rock salt massif may occur at pressure value lower than predicted by micro-fracturing tests carried out in boreholes.

Independently from the above conclusion, in the case of caverns located in homogenic part of the Mogilno salt dome, it is possible to decrease a minimal storage pressure, regardless of current technical projects. However, it is not clear that this improvement could be favourable from the point of view of effective, long-term storage capacity. Only a detailed analysis of exploitation scenario would give the answer.